

Glass-blown spherical microcells for chip-scale atomic devices

E. Jesper Eklund^{a,*}, Andrei M. Shkel^a, Svenja Knappe^b,
Elizabeth Donley^b, John Kitching^b

^a *Microsystems Laboratory, University of California, Irvine, CA 92697-3975, USA*

^b *Time and Frequency Division, National Institute of Standards and Technology, Boulder, CO 80305-3328, USA*

Received 3 April 2007; received in revised form 2 October 2007; accepted 4 October 2007

Available online 10 October 2007

Abstract

This paper demonstrates spherical vapor cells intended to be used in chip-scale atomic devices. A micro glass blowing process is introduced, in which multiple glass spheres are simultaneously shaped on the top of a silicon wafer and subsequently filled with rubidium. In the presented fabrication process, an array of cylindrical cavities is first etched in silicon. Next, a thin glass wafer is anodically bonded to the silicon wafer. The bonded wafers are then placed inside a furnace set to 850 °C. At this elevated temperature, the viscosity of the glass is decreased and the heated trapped gas in the cavities expands, thus causing the glass to be blown into spherical cells. Microscopic alkali vapor cells are achieved by evaporation of ⁸⁷Rb through a small glass nozzle into the cell cavities. The cells are then sealed by anodic bonding. The fabricated cells are characterized and the presence of rubidium vapor inside the cells is verified by observing an absorption spectrum.

© 2007 Elsevier B.V. All rights reserved.

PACS: 07.07.Df; 33.25.+k; 42.81.Pa; 85.85.+j

Keywords: Atomic microdevices; Glass spheres; Microcells; Micro glass blowing; Micromachining; Vapor cells

1. Introduction

Recent advances in the field of atomic microelectromechanical systems (MEMS) have created a need for microscopic alkali metal vapor cells [1–5]. While previous MEMS efforts have been focused primarily on planar vapor cells with only two optical ports [6–9], designed to be used in chip-scale atomic clocks (CSACs) [1] and chip-scale atomic magnetometers (CSAMs) [2], glass-blown spherical cells are traditionally used in macroscopic atomic clocks and other atomic apparatuses. Although glass blowing has in the past been used to achieve millimeter-scale cells (for example [10]), it has not previously been considered a viable option for mass production of microscopic devices.

Spherical vapor cells are preferred in some atomic physics applications in order to minimize the effects of magnetic self-fields generated by the atoms, and to prevent trapping of atoms in the corners of cells that have been coated with antirelaxation coatings [11]. Furthermore, a cell of spherical shape provides

more optical ports than a planar cell, and therefore allows for straightforward pump-probe configurations and enables both vertical and horizontal integration with other MEMS components. The micro glass blowing process presented in this paper was developed as an attempt to address these issues and to facilitate mass production of microscopic spherical gas confinement chambers. These chambers are intended to be used as vapor cells in a micromachined implementation of a nuclear magnetic resonance (NMR) gyroscope. However, the same type of cells may also be utilized in other microfabricated devices, such as atomic magnetometers [2].

In the wafer-level micro glass blowing process, thousands of glass spheres can be shaped simultaneously on top of a silicon wafer [12]. An array of cylindrical cavities is first etched in silicon. Next, a thin glass wafer is anodically bonded to the etched silicon wafer. The bonded wafers are then placed inside a furnace set to 850 °C. Since this temperature is above the softening point of the glass, the viscosity of the glass is decreased. Additionally, the heated trapped gas in the cavities expands, causing the glass to be blown into three-dimensional spherical structures. Once the glass is shaped, the backside of the silicon wafer can be etched and the cells can be filled with various substances [13].

* Corresponding author. Tel.: +1 949 824 0316.

E-mail address: eeklund@uci.edu (E.J. Eklund).

URL: <http://mems.eng.uci.edu> (E.J. Eklund).

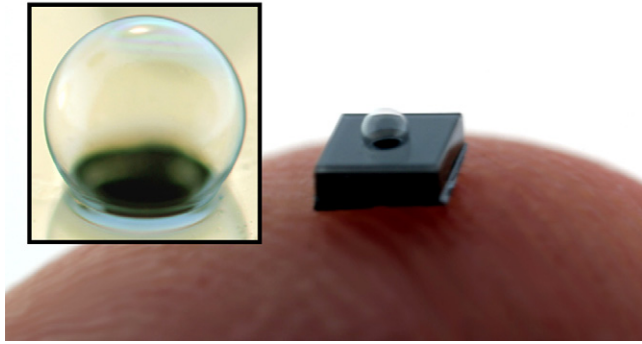


Fig. 1. Diced silicon chip with a side length of 2 mm (on a finger tip). The chip contains a blown glass sphere, shown in the inset picture, with a diameter of approximately 900 μm .

Fig. 1 depicts a fabricated and diced chip containing a blown glass sphere, formed from a 100 μm thick borosilicate glass wafer during three minutes at 850 $^{\circ}\text{C}$. The diameter of the glass sphere is approximately 900 μm .

While the presented glass cells were developed for an NMR gyroscope, we envision that the micro glass blowing process will open the door for a new breed of three-dimensional MEMS. Several applications are envisioned, including mass-produced microscopic glass lenses, spacers for wafer-level packaging, and complex three-dimensional networks for gas analyzers and drug delivery systems.

Section 2 provides a motivation for the use of spherical cells in nuclear magnetic resonance gyroscopes. Next, Section 3 presents the micro glass blowing fabrication process and describes how the cells are filled with rubidium vapor. The experimental setup and the measured rubidium absorption spectrum are then discussed in Section 4.

2. Motivation

The presented glass-blown vapor cells were developed for a micromachined implementation of a nuclear magnetic resonance gyroscope. This section will briefly discuss NMR gyroscopes and why spherical vapor cells are desired in these types of instruments.

Certain noble gas nuclei possess an inherent magnetic moment. These nuclei can be spin-polarized by optically pumping an alkali vapor, which transfers its polarization to the nuclei through a process known as spin exchange [14,15]. When subjected to a static magnetic field, B_0 , the spin-polarized nuclei will precess about the magnetic field lines at the Larmor precession frequency, $\omega_L = \gamma B_0$, where γ is the gyromagnetic ratio. If the Larmor precession is observed in a coordinate frame that rotates at an angular rate ω_R with respect to an inertial frame of reference, the observed frequency will be

$$\omega_{\text{obs}} = \gamma B_0 - \omega_R. \quad (1)$$

This frequency can be detected as a modulation of the light intensity of a circularly polarized beam that is transmitted through the sample, and the angular rate can thus be measured [16,17].

To sustain the Larmor precession in an NMR gyroscope, an oscillating magnetic field must be applied along an axis perpendicular to the B_0 -field at a frequency ω_{AC} , which should be equal to the observed Larmor frequency. The feedback loop will also include a time-dependent white noise component, primarily due to shot noise from random fluctuations of the current in the photodiode used to detect the modulated light intensity. This noise will cause a phase shift between the frequency of the applied magnetic field and the actual Larmor precession frequency. It was shown in [18] that the angle random walk (ARW) of an NMR gyroscope due to this noise is

$$\text{ARW} = \frac{1}{T_2(S/N)\sqrt{\Delta f}} \quad (2)$$

where T_2 is the nuclear spin relaxation time, S/N is the signal-to-noise ratio, and Δf is the bandwidth.

As is the case in all resonance-based instruments, both a large signal-to-noise ratio and a long relaxation time are desired in order to achieve a high-performance gyroscope. Several factors affect the relaxation time of the nuclei, including collisions with the walls of the cell, collisions with other atoms, inhomogeneities of the magnetic field, and the type of noble gas nuclei under consideration [14].

The reduction in relaxation time due to collisions with other atoms and with the cell walls is beyond the scope of this paper. However, wall collisions affect nuclear spins of noble gases considerably less than they affect electron spins of alkali atoms. Relaxation times of several hours have been observed for ^3He spins in large cells made from aluminosilicate glass [19]. In addition, wall coatings can be used to further lengthen the wall-induced relaxation time [20].

If the magnetic field is not perfectly uniform throughout the sample, nuclei at different locations in the cell precess at different frequencies. The uniformity of the applied magnetic field is primarily a technical issue that can be addressed by coil designs of various sophistication, and it is here assumed that a perfectly uniform external field has been applied to the cell. It is well known from classical electrodynamics that the magnetic field inside a uniformly magnetized sphere is $B_M = 2M\mu_0/3$, where M is the magnetization of the sphere and μ_0 is the permeability of free space [21]. The magnetic field inside a uniformly magnetized spherical cell is thus uniform. However, if the cell has a nonspherical shape the magnetic field will be a nonlinear function of location, due to magnetic self-fields generated by the enclosed atoms. In a spherical cell these self-fields cancel out due to symmetry, but in a nonspherical cell the self-magnetization will cause field variations across the sample and can lead to broadening of the magnetic resonance lines [22]. To minimize the effects of self-fields, spherical vapor cells are preferred in high-performance nuclear magnetic resonance gyroscopes.

It should be noted that while this paper focuses on the cell shape, this is only one of many factors that may affect the relaxation time, as was discussed above. Whether or not the magnetic self-field caused by a nonspherical cell shape is the limiting factor depends on the quality of the antirelaxation coating, the amount and type of buffer gas used, and the type of noble gas nuclei under consideration.

3. Fabrication of spherical vapor cells

Nonspherical MEMS alkali vapor cells have previously been fabricated by etching a double-side polished silicon wafer all the way through, followed by anodic bonding of glass wafers to the top and bottom surfaces of the silicon wafer. The cells are filled with the desired substances before the second glass wafer is bonded [6]. These types of vapor cells are an integral part of both chip-scale atomic clocks [1] and chip-scale atomic magnetometers [2]. While the fabrication of the glass-blown spherical vapor cells presented in this section differs from the process used to produce CSAC and CSAM cells, the filling techniques are nearly identical.

3.1. Fabrication process

In conventional glass blowing, a furnace is used to melt a gob of glass. The molten glass is then shaped by repeated blowing and heating steps. Once the desired shapes are achieved, the glass is normally annealed to remove thermal stresses and to prevent the glass from cracking.

The wafer-level micro glass blowing process was designed to emulate conventional glass blowing. However, instead of applying pressure by manual blowing, the increased pressure produced by a heated trapped gas is utilized to shape the glass. While an overview of the fabrication process is presented in this section, a more detailed description and modeling can be found in [12].

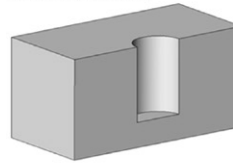
A layer of AZ P4620 [23] photoresist is first patterned on top of a single-crystal silicon wafer. Next, a timed deep reactive ion etch (DRIE) is used to define cylindrical cavities in the silicon, as illustrated in Step 1 in Fig. 2. The photoresist is then removed using acetone and a thin borosilicate glass wafer is anodically bonded to the silicon wafer in air (Step 2). If thin cell walls are desired, the glass may also be ground and polished after it has been bonded to the silicon wafer.

In order to shape the glass, it needs to be heated above its softening point, which occurs at 821 °C for the Pyrex 7740 glass used in the presented process [23,24]. Therefore, in Step 3 of the fabrication process, the bonded wafers are placed inside a furnace at atmospheric pressure and at a temperature of approximately 850 °C. At this elevated temperature, the viscosity of the glass is decreased and the expansion of the heated trapped gas in the cavities thus causes the glass to be blown into spherical shapes. After a few minutes in the furnace the samples are quickly removed to room temperature.

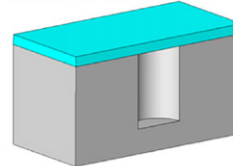
Next, the fabricated glass spheres are annealed in order to remove residual stresses caused by the rapid cool-down of the samples. The Pyrex 7740 [23] glass parts are typically annealed for about 30 min at 560 °C and then slowly cooled to a temperature below the strain point, 510 °C [24].

Fabrication Steps 1–3 in Fig. 2 constitute the foundation of the micro glass blowing process and define the shape and size of the glass structures, as was described in [12]. While these steps are always included in the fabrication process, additional steps can be added as needed to suit a particular application.

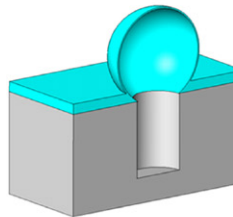
Step 1: Pattern and etch Si wafer



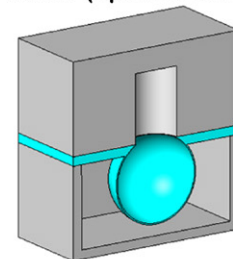
Step 2: Bond Pyrex wafer to Si wafer



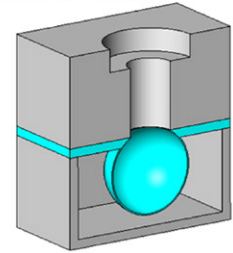
Step 3: Heat in furnace at 850°C



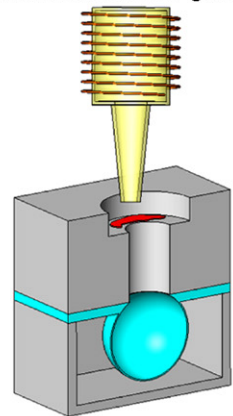
Step 4: Place chip in holder (upside-down)



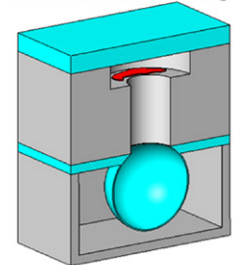
Step 5: Pattern and etch backside



Step 6: Fill cell with alkali and buffer gas



Step 7: Seal backside with anodic bonding



Step 8: Remove chip from holder

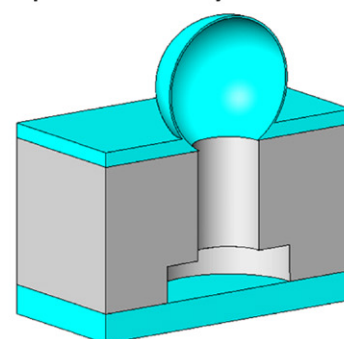


Fig. 2. Fabrication process for spherical glass cells.

In the gas confinement chambers explored in this paper, it is necessary to etch the backside of the silicon wafers in order to be able to fill the glass spheres with an alkali metal and buffer gas. In Step 4, the chip is placed in a temporary holder in order to protect the glass spheres. The backside is then patterned and etched in Step 5, using DRIE.

Different filling techniques have been demonstrated for CSAC and CSAM cells [6–9]. Many of them can also be used to fill the presented glass-blown spherical cells. Here, we choose a filling technique where BaN_6 and $^{87}\text{RbCl}$ are placed inside a small glass ampoule with a 5 mm long nozzle of 700 μm diameter. The chip with the glass-blown cell is placed inside a vacuum chamber and the ampoule is aligned with the cell opening. Next, the ampoule is heated in order to react the compounds, as shown in Step 6 of the fabrication process in Fig. 2. Since the vapor pressure of rubidium is higher than that of Ba and Cl, a fairly pure beam of ^{87}Rb emerges from the ampoule and is deposited into the cell. The nitrogen produced during the reaction is pumped away.

The vacuum chamber is then filled with the desired combination of buffer gases, here a mixture consisting of Xe (natural isotopic abundance) and N_2 . The backside is then sealed by anodic bonding of a glass wafer in Step 7. Finally, the chip is taken out from the vacuum chamber and the temporary holder is removed from the chip in Step 8.

3.2. Size and shape considerations

As was discussed in [12], the volume enclosed by the blown glass sphere can be estimated as

$$V_g = V_e \left(\frac{T_f}{T_s} - 1 \right) \quad (3)$$

where V_e is the volume of the etched cavity, T_f is the furnace temperature, and T_s is the temperature at which the cavities etched in the silicon wafer were sealed by anodic bonding of the glass wafer.

For example, assume that the cavities etched in silicon were sealed at room temperature. Also assume that the chips were placed in a furnace set to 900 °C and at constant atmospheric pressure. Since the temperature inside the furnace is approximately four times higher (1173 K vs. 295 K) than the temperature at which the cavities were sealed, the total enclosed volume (glass sphere + etched cavity) after the glass is blown will be about four times the initial volume (etched cavity). Consequently, the final volume enclosed by only the glass sphere will be three times the volume of the etched cavity, as can be seen from Eq. (3). Geometry considerations can be used to predict the height and radius of the glass spheres, as was described in [12].

It should be noted that while the main part of the cell is spherical, the etched cavity below the glass sphere makes up a significant part of the cell (25% in the example above). It is presently unclear how much this non-spherical part of the cell will affect the relaxation time of the enclosed atoms. However, the volume of this non-spherical part may be reduced by defining structures on the wafer that is used to seal the backside of the cell. Small cylinders designed to fit in the etched cavities may be defined on top of the glass wafer using, for example, a photodefinable glass or polymer. Alternatively, the cavities etched in the silicon wafer can be partially filled with a thermosetting polymer before the glass wafer is bonded to the backside.



Fig. 3. Fabricated array of hollow micro glass spheres.

3.3. Fabricated parts

Single-crystal silicon and borosilicate glass wafers of two-inch diameter were used for the fabrication of the glass spheres. Deep reactive ion etching was used to define an array of cylindrical cavities in a 1 mm thick silicon wafer. The diameter of the cavities was 500 μm and the targeted depth was 750 μm . A borosilicate glass wafer with a thickness of 100 μm was then anodically bonded to the silicon wafer, using a hot plate set to 400 °C and applying a voltage of 600 V. The glass structures were then shaped for about three minutes inside a furnace set to 850 °C and at atmospheric pressure. Fig. 3 shows the resulting fabricated array of glass spheres.

The intended use of the glass spheres is as vapor cells in a nuclear magnetic resonance gyroscope. In this application, both pump and probe light need to be transmitted in two perpendicular directions. To assure that the glass structures are sufficiently smooth, the surface roughness was measured with a confocal microscope (Hyphenated-Systems NanoScale 1500P [23]). The rectangular area marked in Fig. 4(a) was measured in ten different spheres. The measured area for one of the samples is shown in Fig. 4(b). In all samples the average surface roughness was within 12 ± 5 nm. While this is significantly greater than the initial surface roughness of less than 1 nm, specified for the glass wafers, the surfaces are still sufficiently smooth.

4. Experimental results

A fabricated cell was placed inside a transparent thermal chamber and heated to 100 °C in order to obtain sufficient rubidium vapor pressure inside the cell. Next, light was transmitted through the cell by a vertical-cavity surface-emitting laser (VCSEL) with a surrounding thermoelectric cooler (TEC). By controlling the VCSEL temperature and current, the wavelength of the emitted light was tuned. The light was collimated and transmitted through the rubidium vapor cell, and a photodetector was used to measure the intensity of the transmitted light. The experimental setup is shown in Fig. 5. Note that the Helmholtz coils in the experimental setup were not used in the current experiment.

The VCSEL temperature was kept constant at 16 °C and the current was swept from 1.65 mA to 1.75 mA, corresponding to wavelengths of approximately 794.72 nm to 794.80 nm (determined from a VCSEL calibration curve). Fig. 6 displays the

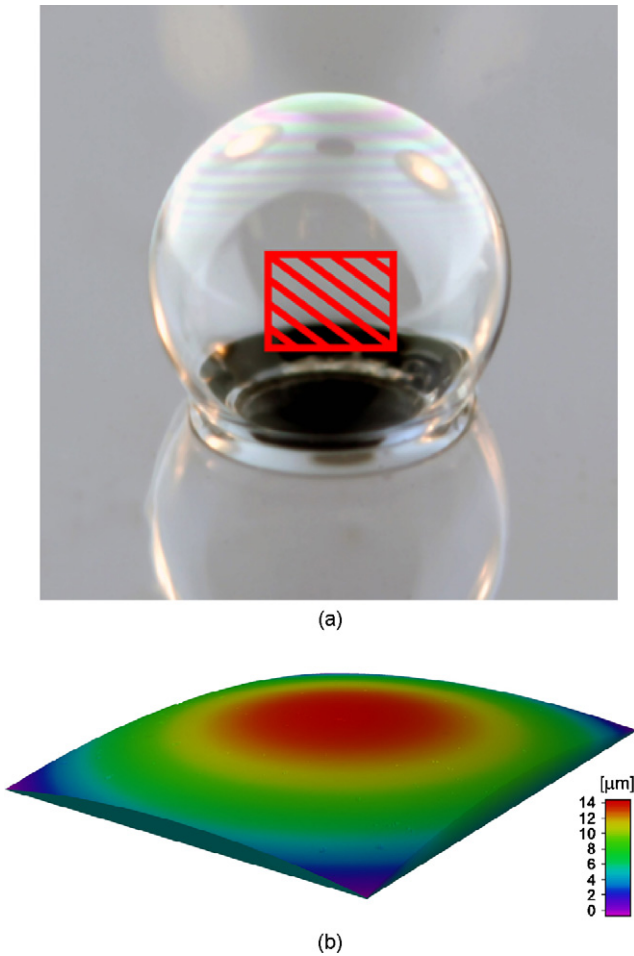


Fig. 4. Surface roughness of glass sphere measured with a confocal microscope. The radius of the sphere is $450\ \mu\text{m}$ and the measured area, marked in (a), is approximately $140\ \mu\text{m} \times 180\ \mu\text{m}$. The color legend in (b) indicates the curvature of this area.

obtained rubidium absorption spectrum. At the wavelength that corresponds to the ^{87}Rb D₁ line (794.76 nm in air) the light is partially absorbed by the rubidium, and the intensity of the transmitted light drops, confirming that the cell contains rubidium 87 vapor. The two overlapped peaks, separated by 6.8 GHz, arise from the hyperfine ground states of ^{87}Rb . This plot veri-

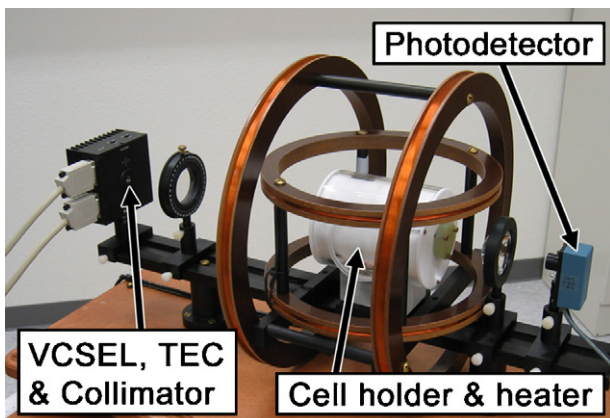


Fig. 5. Experimental setup.

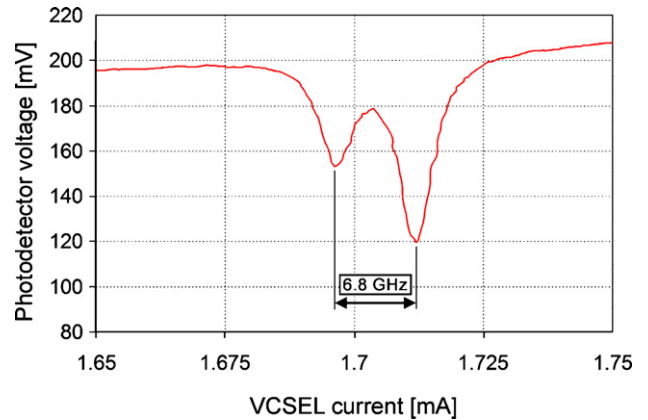


Fig. 6. ^{87}Rb absorption spectrum for VCSEL currents of 1.65 mA ($\sim 794.72\ \text{nm}$) to 1.75 mA ($\sim 794.80\ \text{nm}$).

fies the feasibility of the spherical vapor cells, fabricated by a wafer-level glass blowing process.

It should be noted that a macro-scale heater was used in the experimental setup. If this type of spherical vapor cells are used in microfabricated atomic devices, it is beneficial to have a miniature heater integrated with the cell. For many types of devices, the heater must be designed in such a way that the magnetic fields generated by the heater currents are small (for example [25]). While not yet demonstrated experimentally, several options can be considered for the heater. For example, heater traces can be deposited on the back of the chip. Alternatively, if a material that can withstand the high temperatures required for the glass blowing is used, the heater can potentially be defined on the front side between Steps 2 and 3 in the fabrication process (Fig. 2). Naturally, the heater would now have to be defined in areas of the chip where the glass does not deform. Somewhat more exotic approaches can also be considered, including laser-induced heating, or heat transfer using air or microfluidics.

5. Conclusion

Wafer-level micro glass blowing may enable several MEMS applications, including mass-produced microscopic glass lenses, spacers for wafer-level packaging, and complex three-dimensional networks for gas analyzers and drug delivery systems. One potential application, microscopic gas confinement chambers, was explored in this paper. The need for spherical vapor cells in atomic instruments was addressed by the micro glass blowing process. The feasibility of manufacturing spherical cells was verified and the fabricated samples were shown to contain rubidium vapor.

Acknowledgements

The authors thank Vu Phan of the UCI Integrated Nanosystems Research Facility (INRF) for fabrication support and Dr. Dragos Constantin for technical assistance. The presented research was supported in part by the DARPA NGIMG program. This work is a partial contribution of NIST, an agency of the US government, and is not subject to copyright.

References

- [1] S. Knappe, V. Shah, P. Schwindt, L. Hollberg, J. Kitching, L. Liew, J. Moreland, A microfabricated atomic clock, *Appl. Phys. Lett.* 85 (2004) 1460–1462.
- [2] P. Schwindt, S. Knappe, V. Shah, L. Hollberg, J. Kitching, L. Liew, J. Moreland, Chip-scale atomic magnetometer, *Appl. Phys. Lett.* 85 (2004) 6409–6411.
- [3] R. Lutwak, D. Emmons, T. English, W. Riley, A. Duwel, M. Varghese, D.K. Serkland, G.M. Peake, The chip-scale atomic clock—recent development progress, in: *Proc. 35th Ann. Precise Time and Time Interval Meeting*, San Diego, CA, USA, December 2–4, 2003, pp. 467–478.
- [4] M. Zhu, L.S. Cutler, J.E. Berberian, J.F. DeNatale, P.A. Stupar, C. Tsai, Narrow linewidth CPT signal in small vapor cells for chip scale atomic clocks, in: *Proc. IEEE Intl. Freq. Cont. Symp. and Expo*, Montreal, Canada, August 23–27, 2004, pp. 100–103.
- [5] D.W. Youngner, L.M. Lust, D.R. Carlson, S.T. Lu, L.J. Forner, H.M. Chanvongsak, T.D. Stark, A manufacturable chip-scale atomic clock, in: *Proc. 14th Intl. Conf. Solid-State Sensors, Actuators and Microsystems (Transducers'07)*, Lyon, France, June 10–14, 2007, pp. 39–44.
- [6] L.A. Liew, S. Knappe, J. Moreland, H. Robinson, L. Hollberg, J. Kitching, Microfabricated alkali atom vapor cells, *Appl. Phys. Lett.* 84 (2004) 2694–2696.
- [7] C.-H. Lee, H. Guo, S. Radhakrishnam, A. Lal, C. Szekely, T. McClelland, A.P. Pisano, A batch fabricated rubidium-vapor resonance cell for chip-scale atomic clocks, in: *Proc. Solid-State Sensors, Actuators and Microsystems Workshop (Hilton Head 2004)*, Hilton Head Island, SC, USA, June 6–10, 2004, pp. 23–26.
- [8] F. Gong, Y.-Y. Jau, K. Jensen, W. Happer, Electrolytic fabrication of atomic clock cells, *Rev. Sci. Instrum.* 77 (2006) 076101.
- [9] S. Knappe, V. Gerginov, P.D.D. Schwindt, V. Shah, H.G. Robinson, L. Hollberg, J. Kitching, Atomic vapor cells for chip-scale atomic clocks with improved long-term frequency stability, *Opt. Lett.* 30 (2005) 2351–2353.
- [10] M.V. Balabas, D. Budker, J. Kitching, P.D.D. Schwindt, J.E. Stalnaker, Magnetometry with millimeter-scale antirelaxation-coated alkali–metal vapor cells, *J. Opt. Soc. Am. B* 23 (2006) 1001–1006.
- [11] H.G. Robinson, E.S. Ginsberg, H.G. Dehmelt, Preservation of spin state in free atom–inert surface collisions, *Bull. Am. Phys. Soc.* 3 (1958) 9.
- [12] E.J. Eklund, A.M. Shkel, Glass blowing on a wafer level, *J. Microelectromech. Syst.* 16 (2007) 232–239.
- [13] E.J. Eklund, A.M. Shkel, S. Knappe, E. Donley, J. Kitching, Spherical rubidium vapor cells fabricated by micro glass blowing, in: *Tech. Dig. 20th IEEE Intl. Conf. Micro Electro Mechanical Systems (MEMS 2007)*, Kobe, Japan, January 21–25, 2007, pp. 171–174.
- [14] W. Happer, Optical pumping, *Rev. Mod. Phys.* 44 (1972) 169–250.
- [15] T.G. Walker, W. Happer, Spin-exchange optical pumping of noble-gas nuclei, *Rev. Mod. Phys.* 69 (1997) 629–642.
- [16] J.T. Fraser, Optically pumped magnetic resonance gyroscope and direction sensor, U.S. Patent 3,103,621, 1963.
- [17] K.F. Woodman, P.W. Franks, M.D. Richards, The nuclear magnetic resonance gyroscope: a review, *J. Navigation* 40 (1987) 366–384.
- [18] I.A. Greenwood, J.H. Simpson, Fundamental noise limitations in magnetic resonance gyroscopes, in: *Proc. IEEE 1977 National Aerospace and Electronics Conference (NAECON'77)*, Dayton, OH, USA, May 17–19, 1977, pp. 1246–1250.
- [19] W.A. Fitzsimmons, L.L. Tankersley, G.K. Walters, Nature of surface-induced nuclear-spin relaxation of gaseous ^3He , *Phys. Rev.* 179 (1969) 156–165.
- [20] X. Zeng, E. Miron, W.A. van Wijngaarden, D. Schreiber, W. Happer, Wall relaxation of spin polarized ^{129}Xe nuclei, *Phys. Lett. A* 96 (1983) 191–194.
- [21] J.D. Jackson, *Classical Electrodynamics*, third ed., Wiley, New York, 1999.
- [22] C. Kittel, *Introduction to Solid State Physics*, eighth ed., Wiley, New York, 2005.
- [23] Certain commercial equipment, instruments, or materials are identified in this paper in order to specify the experimental procedure adequately. Such identification is not intended to imply recommendation or endorsement by the National Institute of Standards and Technology, nor is it intended to imply that the materials or equipment identified are necessarily the best available for the purpose.
- [24] Corning, Thermal properties of Corning glasses, 2007. [Online]. Available: http://www.corning.com/lifesciences/technical_information/techdocs/thermalprop.asp.
- [25] P.D.D. Schwindt, B. Lindseth, S. Knappe, V. Shah, J. Kitching, L.A. Liew, A chip-scale atomic magnetometer with improved sensitivity using the Mx technique, *Appl. Phys. Lett.* (2007) 081102.